

The 2<sup>nd</sup> Power and Energy Conversion Symposium (PECS 2014)  
Melaka, Malaysia  
12 May 2014

# Design Study of Single Phase Inner-Rotor Hybrid Excitation Flux Switching Motor For Hybrid Electric Vehicles

Mohamed Mubin Aizat Mazlan, Zhafir Aizat Husin  
Syed Muhammad Naufal Syed Othman and Erwan Sulaiman  
Department of Electric of Power Engineering  
Universiti Tun Hussein Onn Malaysia, Locked Bag 101,  
Batu Pahat, Johor, 86400 Malaysia  
mubinaizat@gmail.com and erwan@uthm.edu.my

**Abstract-** In hybrid excitation machines (HEMs), there are two main flux sources which are permanent magnet (PM) and field excitation coil (FEC). These HEMs have better features when compared with interior permanent magnet synchronous machines (IPMSM) used in conventional hybrid electric vehicles (HEVs). Since all flux sources including PM, FEC and armature coils are located on stator core, the rotor becomes a single piece structure similar with switch reluctance machine (SRM). The combined flux generated by PM and FEC established more excitation fluxes that are required to produce much higher torque of the motor. In addition, variable DC FEC can control the flux capabilities of the motor, thus the machine can be applied for high-speed motor drive system. In this paper, the initial design of single-phase 8S-4P inner-rotor HEFSM is presented. Initially coil arrangement tests are examined to confirm the machine operating principle and position of each armature coil phase. Finally, flux comparison of PM, DC FEC and PM with DC FEC, flux linkage at various FEC current densities,  $J_E$ , flux distribution and flux line of PM with FEC, cogging torque, induced voltage/ back EMF of PM, DC FEC and PM with DC FEC, combination of FEC and armature coil flux characteristic and torque and power versus FEC current density,  $J_E$  at various armature coil current densities,  $J_A$  are also analyzed. As a result, the performance of the initial design motor shows that the maximum torque achieved is 81.6% of the target performance, whereas the maximum power achieved 47.4 kW, 15.6% is greater than the target value. Thus, by further design refinement and optimization it is expected that the motor will successfully achieve the target performances.

## I. INTRODUCTION

By increasing number of population in the world, the demand toward vehicles for personal transportation has also been increased dramatically in the past of decade which leads to serious problems called 'global warming'. One of the main causes of global warming is Internal Combustion Engine (ICE), already used in HEV. Through the report in year 2008 [1], about seven per cent of global carbon dioxide ( $\text{CO}_2$ ) emission in year 2000 came from the vehicles. By the year 2015, it is expected that  $\text{CO}_2$  emission rate from vehicles will increase two times with economic growth.

Hybrid Electric Vehicle (HEV) is considered as an ultimate eco- friendly car and this is highly expected to be popularized in the future [2]. The important of the basic characteristics requirements of an electric motor for HEV drive systems are high torque, high power density, and constant power at high speed as well as high efficiently [3].

Permanent Magnet Synchronous Machine (PMSMs) are used in HEV to overcome problem of low torque density and efficiency [4]. Although PMSM has the advantage of high torque density and high efficiency, still it has the problem of demagnetization and mechanical damage of rotor's magnet. Due to this reason, other alternative machine should be design to overcome the problems of PMSM already installed in HEV.

Then switched reluctance motor (SRM) is invented to overcome the permanent magnet problem. SRM has no PM and robust rotor structure but it is not suitable for HEV due to large torque ripples and noisy [5].

On the other hand, permanent magnet flux switching machine (PMFSM) has been proposed to overcome the problem of PMSM and SRM. This PMFSM has physical compactness, robust rotor structure, higher torque and power density and high efficiency. All magnets are located at the stator which make the temperature of the magnet can easily be controlled [6]. This shows that PMFSM have more advantage when compared with PMSM and SRM [7-10]. The single-phase PMFSM alternator is introduced in 1955 [7] and the three-phase machine is invented in 1997 [10]. The application such as in aircrafts, automotive traction drives, and wind power generation are widely used by using PMFSM design [11-13]. However PMFSM has several disadvantages of uncontrolled flux and high cost.

Recently, many researchers have developed hybrid excitation flux switching machine (HEFSM) for HEV applications. The designed HEFSM consist of permanent magnet (PM) and field excitation coil (FEC) as their main flux sources. HEFSM also consist a robust rotor structure similar with SRM is suitable for extreme driving condition. The PM and FEC are placed at the stator and a simple cooling system can be used for this machines. In addition, FEC place at the

stator can control the variable flux abilities and will make the torque and flux become higher. Several invention of HEFSM for HEV application has been proposed. For example some, 6Slot–5Pole HEFSSM for HEV application has been proposed. Although the proposed machine has met the target performances, the problem of unbalanced pulling force due to odd number of poles is difficult to overcome [14-15]. Besides, 6Slot-8Pole machines also had been proposed but these types of machines have problems of high torque ripple and back-emf waveforms, which are usual concerns for this kind of eight pole machine [16]. It should be noted that all HEFSSM mentioned above are 3-phase HEFSM.

In this paper, the initial design of single-phase 8S-4P inner rotor HEFSM is analysed. Flux comparison of PM, DC FEC and PM with DC FEC, flux linkage at various FEC current densities,  $J_E$ , flux distribution and flux line of PM with FEC, cogging torque, and torque and power versus FEC current density,  $J_E$  at various armature coil current densities,  $J_A$  are also analyzed.

II. DESIGN RESTRICTION AND PARAMETER SPECIFICATIONS OF THE 8S-4P INNER-ROTOR HEFSM  
 In this design study, the motor parameters are divided into two groups, namely, those related to stator iron core and rotor iron core. On the stator iron core, it is subdivided into three components which are the PM shape, FEC slot shape, and armature slot shape. The rotor parameters involved are the inner rotor radius (D1) which is 70% of the size of motor, rotor pole depth (D2) which is the half size of the rotor and rotor pole arc width (D3) is get from the formula  $\sum W_s = \sum W_r$ . The distance between airgap and PM is (D4). The PM slot shape parameters are the PM depth (D5), and the PM width (D6) calculated by using volume of 1kg PM, while for the FEC slot parameters are FEC slot depth and FEC slot width, (D7) and (D8) respectively calculated from Eq 1 using 147.67mm area of FEC.

$$N_a = \frac{J_a \alpha S_a}{I_a} \quad (1)$$

Finally, the armature coil parameters are armature coil slot depth (D9) and the armature coil slot width (D10) calculated from Eq 2 by using 168mm area of armature coil.

$$N_e = \frac{J_e \alpha S_e}{I_e} \quad (2)$$

The motor design parameters, from D1 to D10 are demonstrated in Fig. 1. The parameter specifications and design restriction of the proposed 8S-4P HEFSM are listed in Tables I and II, respectively. From Table I, the rotor parameters such as rotor radius, D1, rotor pole height, D2 and pole width, D3 are set to 92.40mm, 31.20mm and 38.30mm, respectively. Further, the PM depth, D5 is set to 12.55mm while the DC FEC depth and width, D7 and D8 are set to 13.35mm and 10.99mm, respectively. Finally, the armature

coil depth and width, D9 and D10, are set to 26.70mm and 6.29mm, respectively.

From Table II, the electrical restrictions related with the inverter such as maximum 375V DC bus voltage and maximum 360A inverter current are set. The limits of the current densities are set to the maximum of  $30A_{rms}/mm^2$  and  $30A/mm^2$  for armature winding and DC FEC, respectively. In addition, the geometrical dimensions of the HEFSM such as the stator outer diameter, motor stack length, shaft radius and air gap are set to 264mm, 70mm, 30mm and 0.8mm respectively, while the PM weight is set to be 1.0kg. The target performance for maximum torque and power are 111Nm and 41kW respectively.

TABLE I  
 OUTER ROTOR DESIGN PARAMETER OF 8S-4P HEFSM

Parameter	Description	Outer-rotor HEFSM
D <sub>1</sub>	Rotor outer radius (mm)	92.40
D <sub>2</sub>	Rotor pole depth (mm)	31.20
D <sub>3</sub>	Rotor pole width (mm)	38.80
D <sub>4</sub>	Distance of airgap (mm)	0.80
D <sub>5</sub>	PM depth (mm)	12.55
D <sub>6</sub>	PM width (mm)	8.86
D <sub>7</sub>	FEC slot depth (mm)	13.35
D <sub>8</sub>	FEC slot width (mm)	10.99
D <sub>9</sub>	AC slot depth (mm)	26.70
D <sub>10</sub>	AC slot width (mm)	6.29

TABLE II  
 HEFSM DESIGN RESTRICTIONS

Items	Unit	8S-4P HEFSSM
Max. DC-bus voltage inverter	V	375
Max. inverter current	A <sub>rms</sub>	360
Max. current density in armature winding, $J_a$	A <sub>rms</sub> /mm <sup>2</sup>	30
Max. current density in excitation winding, $J_e$	A/mm <sup>2</sup>	30
Stator outer diameter	mm	264
Motor stack length	mm	70
Shaft radius	mm	30
Air gap length	mm	0.80
PM weight	kg	1
Maximum speed	r/min	1200
Maximum torque	Nm	>111
Maximum power	kW	>41
Area of FEC	mm <sup>2</sup>	147.67
Area of armature coil	mm <sup>2</sup>	168
FEC coil number	turns	44
Armature coil number	turns	7

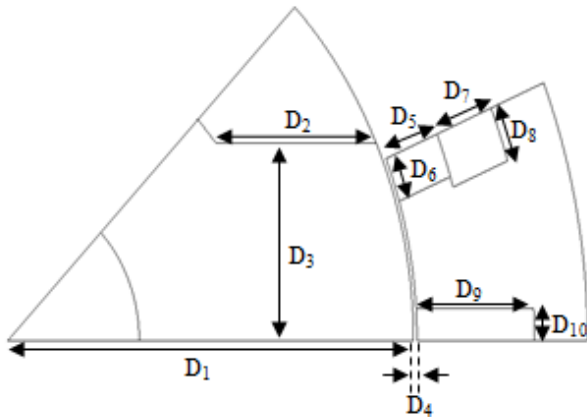


Fig. 1. Design parameter of inner rotor HEFSM

Fig. 2 shows the cross sectional view of initial design of 8S-4P inner-rotor HEFSM.

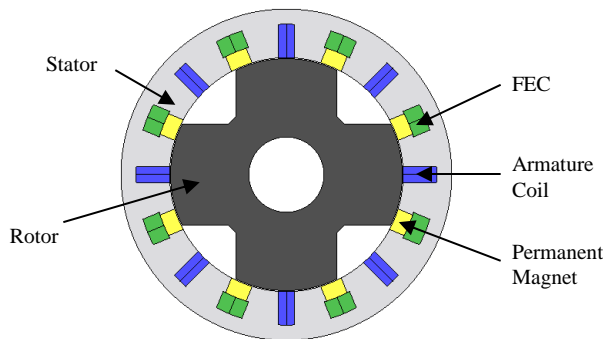


Fig. 2. Initial design of 8S-4P of inner rotor HEFSM

### III. PERFORMANCE PREDICTIONS OF THE 8S-4P OUTER-ROTOR HEFSM BASED ON 2D-FEA

#### A. Flux Armature Coil Arrangement Test of PM Flux

The arrangement of 8 armature coil is tested using coil test analysis to the proposed inner-rotor HEFSM. All armature coils are set in alternate direction. Then, the flux linkage in each armature coil slot is analyzed. From the analysis, it is found that all armature coil slots produce one phase of flux linkage and produce the maximum flux of 0.04mWb. Then all the flux same pattern of armature coil combined to form a total single flux of PM only as shown in Fig.3. The flux of combination 8 armature coils is 0.29mWb proving that the flux become 8 times higher than the single armature coil.

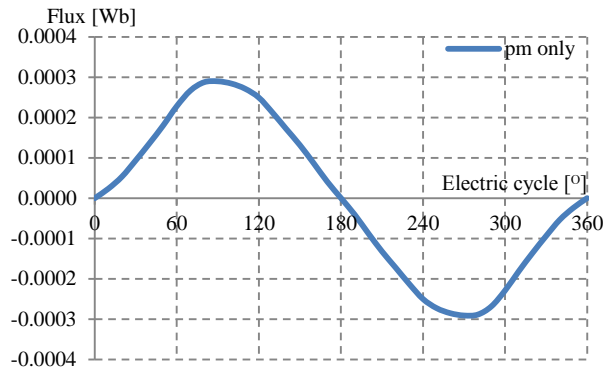


Fig.3. Flux linkage produced by PM only

#### B. Flux Comparison of PM, DC FEC and PM with DC FEC

Fig. 4. show the flux interaction of PM, DC FEC and PM with DC FEC for inner-rotor HEFSM. The maximum flux for PM is 0.29mWb and the maximum flux for DC FEC is 55.62mWb. When PM flux is combined with the DC FEC, the flux linkage become 65.90mWb and the flux become higher compared to PM only or FEC only. This show that the flux from PM has been successfully interacts with the FEC flux without any leakage.

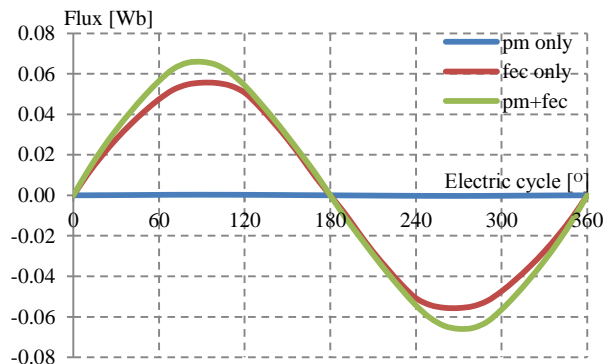


Fig.4. Flux comparison of PM,DC FEC and PM with DC FEC

#### C. Flux linkage at various FEC current densities, $J_E$

PM with FEC flux linkage graph at various FEC current densities,  $J_E$  show the comparison of PM with FEC at various  $J_E$  current.  $J_E$  are varies from 5 to 30A/mm<sup>2</sup> and the number of FEC coil is 44. In Fig.5, the maximum flux linkage of PM with DC FEC at 30A/mm<sup>2</sup>. The flux linkage increase from DC FEC current 5A/mm<sup>2</sup> until 30A/mm<sup>2</sup>. Fig.6 show maximum flux of PM with DC FEC. The maximum flux linkage obtained is approximately 65.90mWb. The outer-rotor HEFSM flux increase when higher DC FEC current density is injected to the system. There is no flux cancellation occur in the stator core.

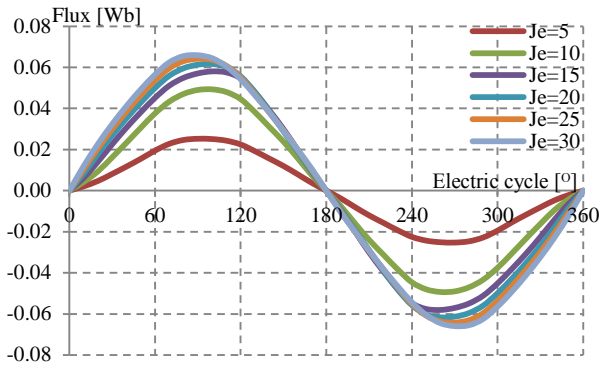


Fig.5. PM with FEC flux linkage at various FEC current densities,  $J_E$

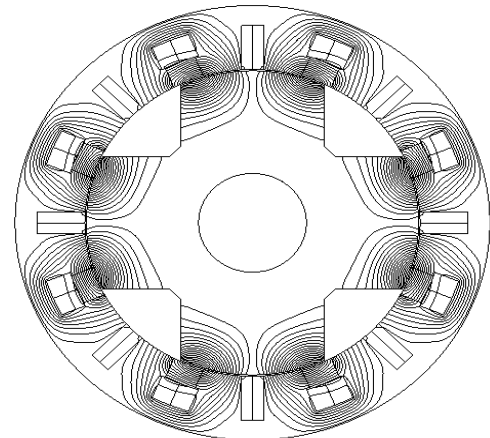


Fig.7. Flux line of PM with FEC

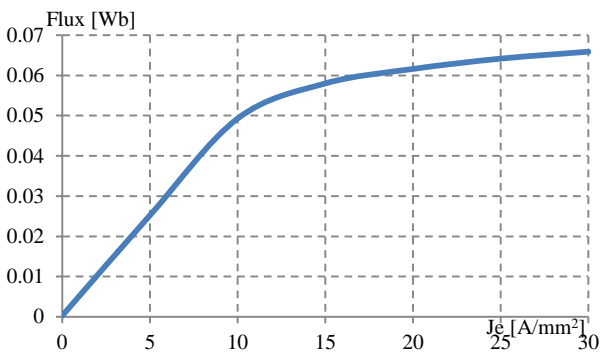


Fig.6. Maximum flux of PM with DC FEC at various FEC current densities,  $J_E$

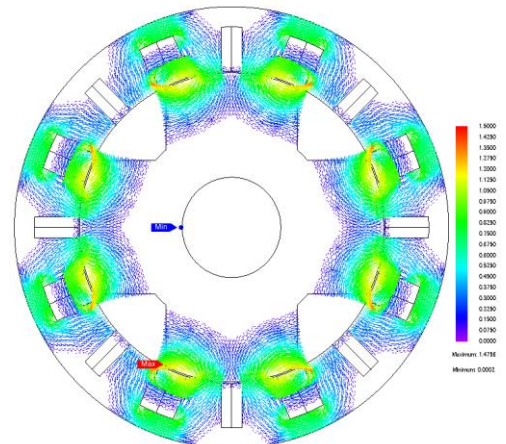


Fig.8. Flux distribution of PM with FEC

#### D. Flux Distribution and Flux Line of PM with FEC

The flux lines and flux distribution at zero rotor position of PM with DC FEC for inner-rotor 8S-4P HEFSMs are illustrated in Fig.7. It is clear that all flux lines flow from stator to rotor and return to armature coil itself. The combined flux generated by PM and FEC established more excitation fluxes that are required to produce higher torque of the motor. Meanwhile, flux distribution in Fig.8 shows the minimum and the maximum flux density of the motor. The red indicator shows the maximum flux density which is at 1.47Wb while the blue indicator shows the minimum flux density which is at 2mWb.

#### E. Cogging Torque

Fig.9 shows the cogging torque profile of PM flux only. Two cycles is formed as the rotor being rotate 360° electric cycle. The cogging torque generated is low which is good for the motor to produce low torque ripples. The maximum peak-to-peak of cogging torque is 0.0032 Nm.

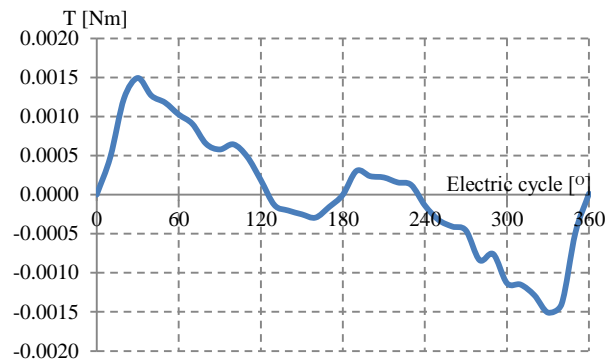


Fig.9. Cogging torque profile on PM only

*F. Induced Voltage/ Back EMF of PM, DC FEC and PM with DC FEC*

Induced voltage or back EMF is electromagnetic force appearing in an inductive circuit in such a direction as to oppose any change of current in the circuit. The induced voltage of inner-rotor 8S-4P HEFSM at PM only, DC FEC only at maximum  $J_E$  of 30 A/mm<sup>2</sup> and PM with DC FEC only at maximum  $J_E$  of 30 A/mm<sup>2</sup> is illustrated in Fig.10. The voltages fundamental and harmonic are shown in the graph. The induced voltage generated from the flux of PM only is 0.14V and is slightly sinusoidal. At DC FEC only where maximum  $J_E$  of 30 A/mm<sup>2</sup> is applied, the induced voltage is much distorted approximately 31.06V due to the strengthening effect by the FEC flux. Meanwhile for PM with DC FEC only at maximum  $J_E$  of 30 A/mm<sup>2</sup>, the distortion of induced voltage is reduced due to flux cancellation of PM and FEC

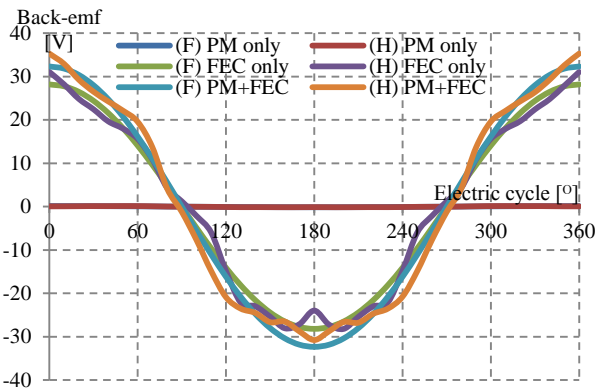


Fig.10. Induced voltage/ back EMF of PM, DC FEC and PM with DC FEC

*G. Resultant Flux of Combination FEC and Armature Coil Flux Characteristic*

The resultant flux is produced from the combination of FEC and armature coil current. Fig.11 shows the resultant flux for inner-rotor 8S-4P HEFSM. There are the graph of the reaction between PM only, FEC flux  $J_E$  of 30 A/mm<sup>2</sup>,  $J_A$  of 30 A/mm<sup>2</sup> and the resultant flux  $J_A$  of 30 A/mm<sup>2</sup>,  $J_E$  of 30 A/mm<sup>2</sup> with shifted angle of 20°. There is a distortion for the resultant flux produce due to the flux cancellation and flux loss during the flux switching from stator to rotor and vice versa.

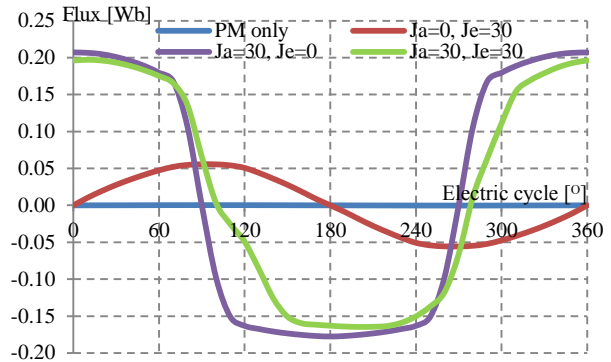


Fig.11. Resultant flux of 8S-4P HEFSM

*H. Torque and Power Versus FEC Current Densities,  $J_E$  at Various Armature Coil Current Densities,  $J_A$*

In load analysis, both FEC and armature coil current are supplied in the circuit with the values that have been calculated. From the torque value, the power value can be obtained. Both  $J_A$  and  $J_E$  are varied from 5A/mm<sup>2</sup> to 30A/mm<sup>2</sup> and 5Arms/mm<sup>2</sup> to 30Arms/mm<sup>2</sup>, respectively. Fig.12 and Fig.13 show the torque and power versus  $J_E$  at various  $J_A$ , respectively. The plots clearly show that the maximum torque of inner-rotor HEFSM is 90.61Nm while the average instantaneous power is 47.44kW obtained when armature coil and DC FEC current densities are set to the maximum of 30Arms/mm<sup>2</sup> and 30A/mm<sup>2</sup>. The torque and power is directly proportional to each other. From both graph, when  $J_A$  increase, the torque and the power increase smoothly. So the motor is in good condition thus the performance of motor will be increase. This shows that the torque and power are directly proportional to the armature coil current densities.

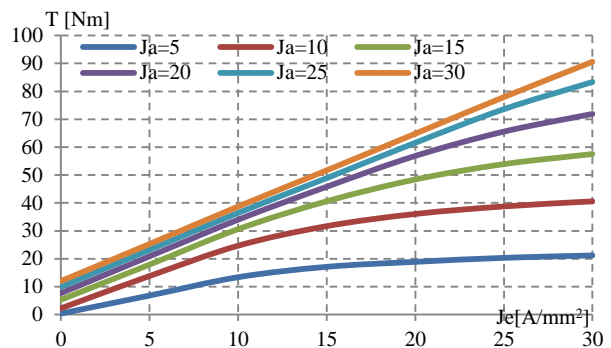


Fig.12. Torque graph against  $J_E$  at various  $J_A$

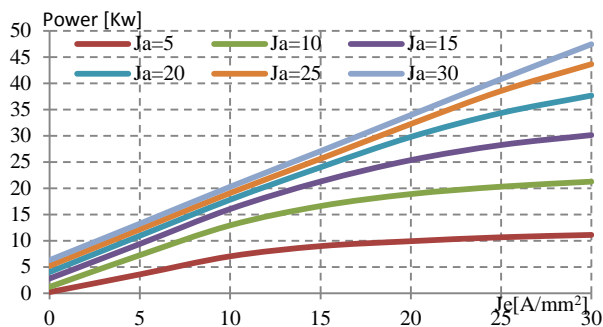


Fig.13. Power graph against  $J_g$  at various  $J_a$

#### IV. CONCLUSIONS

In this paper, a novel 8Slot-4Pole of inner-rotor HEFSM with PM, FEC and armature windings located in the stator are proposed based on the flux switching topology. The maximum torque achieved is 81.6% of the target performance, whereas the maximum power has achieved 47.4 kW which 15.6% is greater than the target value. Although the 8S-4P motor is only the initial design, the torque achieved is considered acceptable and suitable for the single-phase applications. However, design optimization on inner-rotor HEFSM will be conducted in future.

#### V. ACKNOWLEDGEMENT

This research was supported by GIPS (1369) under Research, Innovation, Commercialization and Consultancy Management (ORICC) UTHM, BatuPahat and Ministry of Higher Education Malaysia (MOHE)

#### VI. REFERENCES

- [1] M. Z. Ahmad, E. Sulaiman, Z. A. Haron, and T. Kosaka, "Impact of rotor pole number on the characteristics of outer-rotor hybrid excitation flux switching motor for in-wheel drive EV", Proc of Int. Conf on Electrical Eng. &Infor., UKM, 24-25 June 2013.
- [2] M. Z. Ahmad, E. Sulaiman, Z. A. Haron, and T. Kosaka, "Design improvement of a new outer-rotor hybrid excitation flux switching motor for in-wheel drive EV", IEEE Int. Power Engineering and Optimization Conference, Langkawi, June 2013.
- [3] M. Z. Ahmad, E. Sulaiman, Z. A. Haron and T. Kosaka, "Preliminary Studies on Permanent Magnet Flux Switching Machine with Hybrid Excitation Flux for Direct Drive Electric Vehicle Application", IEEE Int. Conf. on Power and Energy (PECON-2012), Sabah, Dec 2012
- [4] W. Fei, P. Luk, and K. Jinupun, "A New Axial flux magnet segmented- armature-torus machine for in-wheel direct drive applications," IEEE Power Electronics Specialist Conference, pp. 2197-2202, 2008.
- [5] M. Z. Ahmad, E. Sulaiman, Z. A. Haron and T. Kosaka, "A New Structure of Outer-Rotor PMFSM with Hybrid Excitation Flux for In-Wheel Drive EV Applications", Proc.

The 5th Int. Conference on Postgraduate Education (ICPE-5 2012), UTM, Dec 2012

- [6] M. Z. Ahmad, E. Sulaiman, Z. A. Haron, and T. Kosaka, "Design improvement of a new outer-rotor hybrid excitation flux switching motor for in-wheel drive EV", IEEE Int. Power Engineering and Optimization Conference, Langkawi, June 2013.
- [7] S. E. Rauch and L. J. Johnson, "Design principles of flux switch alternators," AIEE Trans., vol 74III, no. 12, pp. 1261-1269, 1955.
- [8] Y. Chen, S. Chen, Z.Q. Zhu, D. Howe, and Y.Y. Ye, "Starting torque of single phase flux switching permanent magnet motors," IEEE Trans. Magn., vol 42, no. 10, pp. 3416-3418, 2006.
- [9] E. Hoang, M. Lecrivain, and M. Gabsi, "A New Structure of a Switching Flux Synchronous Polyphased Machine," in *European Conference on Power Electronics and Applications*, no. 33, pp. 1-8, 2007.
- [10] E. Hoang, A. H. Ben-Ahmed, and J. Lucidarme, "Switching Flux PM Polyphased synchronous machine," in Proc. 7th Eur Conf. Power Electronics Appl., Sept 1997, pp. 903-908.
- [11] Y. Amara, E. Hoang, M. Gabsi, and M. Lecrivain, "Design and comparison of different flux-switching synchronous machines for an aircraft oil breather application," Euro. Trans Electr. Power, no. 15, pp. 497-511, 2005.
- [12] M. Z. Ahmad, E. Sulaiman, M. Jenal, W. M. Utomo, S. A. Zulkifli, A. A Bakar, "Design Investigation of Three Phase HEFSM with Outer-Rotor Configuration " IEEE Conf. on Clean Energy & Technology, 18-20 Nov 2013
- [13] E. Sulaiman, M. Z. Ahmad, T. Kosaka, and N. Matsui, "Design Optimization Studies on High Torque and High Power Density Hybrid Excitation Flux Switching Motor for HEV", *Procedia Engineering*, Vol. 53, pp. 312-322, Mar 2013.
- [14] E. Sulaiman, T. Kosaka, and N. Matsui, "Design Optimization and Performance of a Novel 6- Slot 5-Pole PMFSM with Hybrid Excitation for Hybrid Electric Vehicle", *IEEEJ Transaction on Industry Application*, Vol. 132 / No. 2 / Sec. D pp. 211-218, Jan 2012. (Scopus)
- [15] E. Sulaiman, T. Kosaka, and N. Matsui, "Design and Performance of 6-Slot 5-Pole Permanent Magnet Flux Switching Machine with Hybrid Excitation for Hybrid Electric Vehicle Applications", Proc. The 2010 International Power Electronics Conference, (IPEC 2010), Sapporo (Japan), June 2010.
- [16] E. Sulaiman, T. Kosaka, and N. Matsui, "High power density design of 6S-16P permanent magnet flux switching machine with field excitation for hybrid electric vehicles", *Journal of Power Electronics and Motion Control*, Vol.3, No.1, pp.24-30, Feb 2011.